Article

Targeted Proton Delivery in the Catalyzed Reduction of Oxygen to Water by Bimetallic Pacman Porphyrins

Christopher J. Chang, Zhi-Heng Loh, Chunnian Shi, Fred C. Anson, and Daniel G. Nocera

J. Am. Chem. Soc., **2004**, 126 (32), 10013-10020• DOI: 10.1021/ja049115j • Publication Date (Web): 14 July 2004

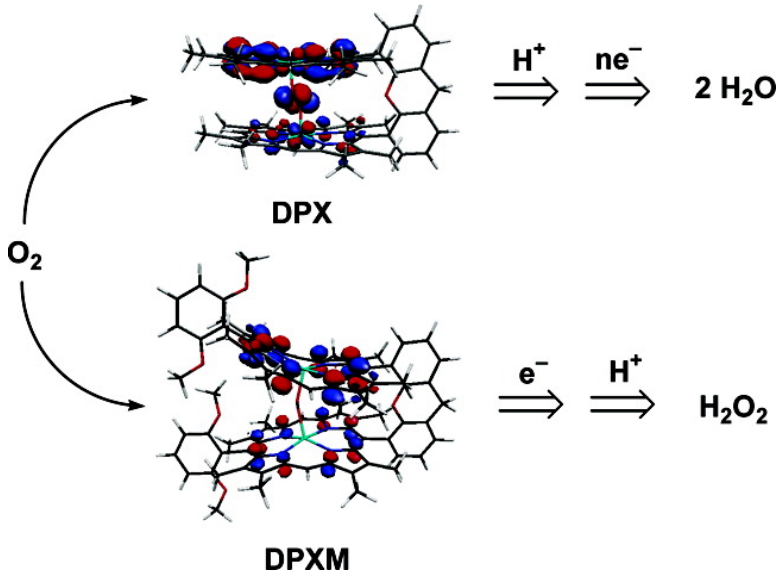

More About This Article

Additional resources and features associated with this article are available within the HTML version:

- Supporting Information
- Links to the 15 articles that cite this article, as of the time of this article download
- Access to high resolution figures
- Links to articles and content related to this article
- Copyright permission to reproduce figures and/or text from this article

View the Full Text HTML

J|A|C|S
ARTICLES
Published on Web 07/14/2004

Targeted Proton Delivery in the Catalyzed Reduction of Oxygen to Water by Bimetallic Pacman Porphyrins

Christopher J. Chang,† Zhi-Heng Loh,† Chunnian Shi,‡ Fred C. Anson,*,‡ and Daniel G. Nocera*,†

Contribution from the Department of Chemistry, 6-335, Massachusetts Institute of Technology, 77 Massachusetts Avenue, Cambridge, Massachusetts 02139, and Division of Chemistry and Chemical Engineering, Arthur Amos Noyes Laboratory, California Institute of Technology, Pasadena, California 91125

Received February 17, 2004; E-mail: nocera@mit.edu

Abstract: A combined experimental and theoretical investigation of the role of proton delivery in determining O_2 reduction pathways catalyzed by cofacial bisporphyrins is presented. A homologous family of dicobalt(II) Pacman porphyrins anchored by xanthene [Co_2(DPX) (**1**) and Co_2(DPXM) (**3**)] and dibenzofuran [Co_2(DPD) (**2**) and Co_2(DPDM) (**4**)] have been synthesized, characterized, and evaluated as catalysts for the direct four-proton, four-electron reduction of O_2 to H_2O. Structural analysis of the intramolecular diiron(III) μ-oxo complex Fe_2O(DPXM) (**5**) and electrochemical measurements of **1**−**4** establish that Pacman derivatives bearing an aryl group trans to the spacer possess structural flexibilities and redox properties similar to those of their parent counterparts; however, these trans-aryl catalysts exhibit markedly reduced selectivities for the direct reduction of O_2 to H_2O over the two-proton, two-electron pathway to H_2O_2. Density functional theory calculations reveal that trans-aryl substitution results in inefficient proton delivery to O_2-bound catalysts compared to unsubstituted congeners. In particular, the HOMO of $[Co_2(DPXM)(O_2)]^+$ disfavors proton transfer to the bound oxygen species, funneling the O−O activation pathway to single-electron chemistry and the production of H_2O_2, whereas the HOMO of $[Co_2(DPX)(O_2)]^+$ directs protonation to the $[Co_2O_2]$ core to facilitate subsequent multielectron O−O bond activation to generate two molecules of H_2O. Our findings highlight the importance of controlling both proton and electron inventories for specific O−O bond activation and offer a unified model for O−O bond activation within the clefts of bimetallic porphyrins.

Introduction

Cytochrome *c* oxidase (COX) and related heme/copper terminal oxidases are the fuel cells of aerobic organisms. These enzymes catalyze the selective and complete four-proton, four-electron conversion of oxygen to water without releasing partially reduced peroxide (or superoxide) intermediates that are toxic to cells.[1−7] COX is distinguished structurally from other heme-dependent proteins of O_2 metabolism, owing to the presence of an essential copper metal center proximate to the heme cofactor. The catalytic reaction cycle of O_2 reduction by the bimetallic heme/Cu_B active site of COX appears, however, to proceed through heme-oxygen intermediates that are similar to those observed in monometallic heme enzymes.[8−11] The precise role for Cu_B in mediating O_2 reduction thus remains unresolved.

The role of a second proximate metal site for achieving selective proton-coupled reduction of O_2 to H_2O in synthetic bimetallic catalysts is also yet to be determined.[12−16] Several porphyrin templates bearing a distal metal-binding cap catalyze the direct four-proton, four-electron reduction of O_2 to H_2O at physiological pH with high selectivity over the more common two-proton, two-electron pathway to afford H_2O_2.[17−25] These

† Massachusetts Institute of Technology.
‡ California Institute of Technology

(1) Babcock, G. T.; Wikström, M. *Nature* **1992**, *356*, 301−309.
(2) Ferguson-Miller, S.; Babcock, G. T. *Chem. Rev.* **1996**, *96*, 2889−2907.
(3) Wikström, M. *Biochim. Biophys. Acta* **2000**, *1458*, 188−198.
(4) Malmström, B. G. In *Electron Transfer in Chemistry*; Balzani, V., Ed.; Wiley-VCH: Weinheim, Germany, 2001; Vol. 3.1.3, pp 39−55.
(5) Brzezinski, P.; Larsson, G. *Biochim. Biophys. Acta* **2003**, *1605*, 1−13.
(6) Schultz, B. E.; Chan, S. I. *Annu. Rev. Biophys. Biomol. Struct.* **2001**, *30*, 23−65.
(7) Michel, H.; Behr, J.; Harrenga, A.; Kannt, A. *Annu. Rev. Biophys. Biomol. Struct.* **1998**, *27*, 329−356.
(8) Witt, S. N.; Chan, S. I. *J. Biol. Chem.* **1987**, *262*, 1446−1448.
(9) Proshlyakov, D. A.; Pressler, M. A.; Babcock, G. T. *Proc. Natl. Acad. Sci. U.S.A.* **1998**, *95*, 8020−8025.
(10) Fabian, M.; Wong, W. W.; Gennis, R. G.; Palmer, G. *Proc. Natl. Acad. Sci. U.S.A.* **1999**, *96*, 13114−13117.
(11) Gennis, R. B. *FEBS Lett.* **2003**, *555*, 2−7.
(12) Collman, J. P.; Boulatov, R.; Sunderland, C. J.; Fu, L. *Chem. Rev.* **2004**, *104*, 561−588.
(13) Kim, E.; Chufán, E. E.; Kamaraj, K.; Karlin, K. D. *Chem. Rev.* **2004**, *104*, 1077−1134.
(14) Gavrilova, A. L.; Bosnich, B. *Chem. Rev.* **2004**, *104*, 349−384.
(15) Gavrilova, A. L.; Qin, C. J.; Sommer, R. D.; Rheingold, A. L.; Bosnich, B. *J. Am. Chem. Soc.* **2002**, *124*, 1714−1722.
(16) Naruta, Y.; Sasaki, T.; Tani, F.; Tachi, Y.; Kawato, N.; Nakamura, N. *J. Inorg. Biochem.* **2001**, *83*, 239−246.
(17) Collman, J. P.; Fu, L.; Herrmann, P. C.; Zhang, X. *Science* **1997**, *275*, 949−951.
(18) Collman, J. P.; Fu, L.; Herrmann, P. C.; Wang, Z.; Rapta, M.; Bröring, M.; Schwenninger, R.; Boitrel, B. *Angew. Chem., Int. Ed.* **1998**, *37*, 3397−3400.
(19) Collman, J. P.; Rapta, M.; Bröring, M.; Raptova, L.; Schwenninger, R.; Boitrel, B.; Fu, L.; L'Her, M. *J. Am. Chem. Soc.* **1999**, *121*, 1387−1388.
(20) Boulatov, R.; Collman, J. P.; Shiryaeva, I. M.; Sunderland, C. J. *J. Am. Chem. Soc.* **2002**, *124*, 11923−11935.
(21) Ricard, D.; Andrioletti, B.; L'Her, M.; Boitrel, B. *Chem. Commun.* **1999**, 1523−1524.

Chart 1

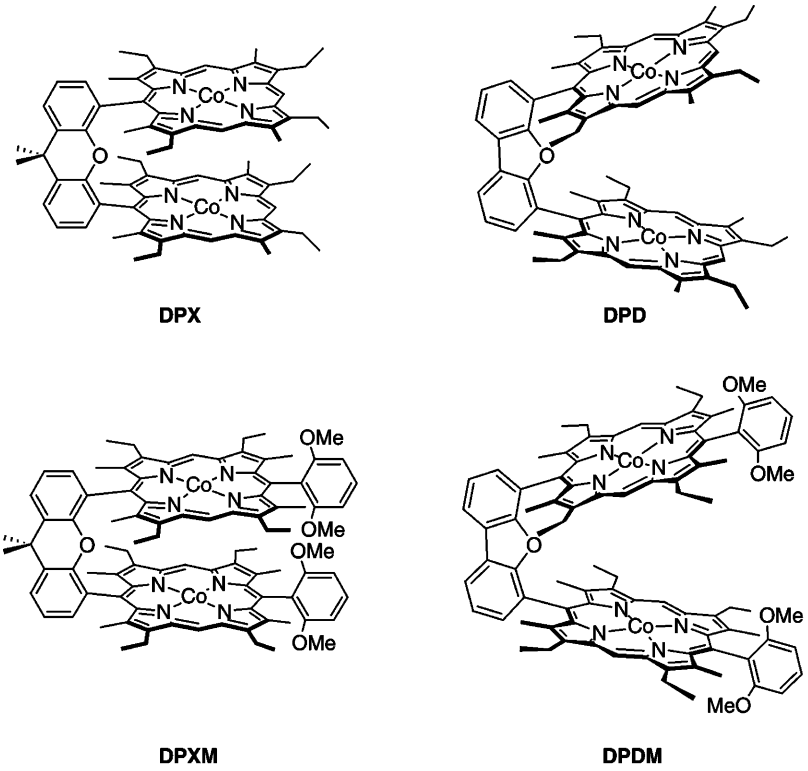

catalysts exhibit comparable selectivities for the four-proton, four-electron pathway *with* or *without* a second redox-active metal ion bound in the distal cap.[20−23] In addition, cofacial Pacman porphyrins containing two cobalt centers,[26,27] one cobalt and one Lewis acidic metal,[28] or one cobalt and one metal-free subunit[29,30] are all effective catalysts for the direct production of H_2O from O_2.

Taken together, the results from these biological and synthetic catalysts imply that the selective reduction of O_2 to H_2O over H_2O_2 steps beyond the idea of simple redox cooperativity between proximate metal centers. Noting that O_2 reduction requires both proton and electron equivalents, we sought to interrogate the role of proton delivery in determining O_2 reduction pathways catalyzed by bimetallic systems. In this report, we present experimental and theoretical studies of the proton-coupled O_2 reduction chemistry catalyzed by a family of dicobalt(II) cofacial bisporphyrins. The structural and redox properties, catalytic behavior, and electronic structures of bimetallic Pacman porphyrins anchored by xanthene (DPX = diporphyrin xanthene) and dibenzofuran (DPD = diporphyrin dibenzofuran) are compared to those of analogues that bear an aryl group trans to the spacer (DPXM = diporphyrin xanthene methoxyaryl, DPDM = diporphyrin dibenzofuran methoxyaryl). The results obtained from X-ray structural analysis, electrochemistry, and the electrocatalytic reduction of O_2, together with density functional theory calculations, identify critical structural and electronic features that govern the selectivity for O_2 reduction. We find that installation of a trans-aryl group into the Pacman motif leads to an appreciably decreased selectivity for the four-proton, four-electron pathway by diverting the delivery of a proton to the $[Co_2O_2]$ core. Our results show that targeted proton delivery is required for the direct reduction of O_2 to H_2O catalyzed by cofacial bisporphyrins and provide a basis for designing systems for selective bond-making and bond-breaking catalysis by proton-coupled electron transfer (PCET).

Results

Synthesis and Structural Chemistry. Dicobalt(II) complexes of the four Pacman systems DPX,[31,32] DPXM,[33] DPD,[32,34] and DPDM[33] (Chart 1) are obtained by reaction of the corresponding free base bisporphyrins with $CoCl_2$ in the presence of 2,6-lutidine.[27] Purification by column chromatography in an inert atmosphere followed by recrystallization furnishes homobimetallic complexes Co_2(DPX) (**1**), Co_2(DPD) (**2**), Co_2(DPXM) (**3**),

(22) Ricard, D.; Didier, A.; L'Her, M.; Boitrel, B. *ChemBioChem* **2001**, *2*, 144−148.
(23) Ricard, D.; L'Her, M.; Richard, P.; Boitrel, B. *Chem. Eur. J.* **2001**, *7*, 3291−3297.
(24) Didier, A.; L'Her, M.; Boitrel, B. *Org. Biomol. Chem.* **2003**, *1*, 1274−1276.
(25) Shin, H.; Lee, D.-H.; Kang, C.; Karlin, K. D. *Electrochim. Acta* **2003**, *48*, 4077−4082.
(26) Chang, C. K.; Liu, H. Y.; Abdalmuhdi, I. *J. Am. Chem. Soc.* **1984**, *106*, 2725−2726.
(27) Chang, C. J.; Deng, Y.; Shi, C.; Chang, C. K.; Anson, F. C.; Nocera, D. G. *Chem. Commun.* **2000**, 1355−1356.
(28) Guilard, R.; Brandès, S.; Tardieux, C.; Tabard, A.; L'Her, M.; Miry, C.; Gouerec, P.; Knop, Y.; Collman, J. P. *J. Am. Chem. Soc.* **1995**, *117*, 11721−11729.
(29) Lui, H.-Y.; Abdalmuhdi, I.; Chang, C. K.; Anson, F. C. *J. Phys. Chem.* **1985**, *89*, 665−670.
(30) Ni, C.-L.; Abdalmuhdi, I.; Chang, C. K.; Anson, F. C. *J. Phys. Chem.* **1987**, *91*, 1158−1166.
(31) Chang, C. J.; Deng, Y.; Heyduk, A. F.; Chang, C. K.; Nocera, D. G. *Inorg. Chem.* **2000**, *39*, 959−966.
(32) Chang, C. J.; Baker, E. A.; Pistorio, B. J.; Deng, Y.; Loh, Z.-H.; Miller, S. E.; Carpenter, S. D.; Nocera, D. G. *Inorg. Chem.* **2002**, *41*, 3102−3109.
(33) Chang, C. J.; Deng, Y.; Lee, G.-H.; Peng, S.-M.; Yeh, C.-Y.; Nocera, D. G. *Inorg. Chem.* **2002**, *41*, 3008−3016.
(34) Deng, Y.; Chang, C. J.; Nocera, D. G. *J. Am. Chem. Soc.* **2000**, *122*, 410−411.

Table 1. Crystallographic Data for Fe_2O(DPXM) (**5**)

empirical formula	$C_{105}H_{122}Cl_8Fe_2N_8O_6$
fw	1987.41
temp	183(2) K
wavelength	0.71073 Å
cryst syst	triclinic
space group	$P\bar{1}$
unit cell dimensions	$a = 15.1206(6)$ Å
	$b = 16.0783(7)$ Å
	$c = 24.5229(11)$ Å
	$\alpha = 72.500(1)°$
	$\beta = 79.253(1)°$
	$\gamma = 66.396(1)°$
vol	5195.3(4) Å^3
Z	2
density (calculated)	1.270 Mg/m^3
abs coeff	0.540 mm^{-1}
F(000)	2088
cryst size	0.36 mm × 0.11 mm × 0.10 mm
θ range for data collection	2.37−25.00°
reflns collected	23352
independent reflns	17671 [R(int) = 0.0387]
data/restraints/parameters	17671/14/1144
GOF on F^2	1.051
final R indices [$I > 2\sigma(I)$]	$R1 = 0.0858$
	w$R2 = 0.2103$
R indices (all data)	$R1 = 0.1311$
	w$R2 = 0.2496$
largest diff peak	1.554 e Å^{-3}
largest diff hole	−0.787 e Å^{-3}

and Co_2(DPDM) (**4**) in excellent yields (>90%). The steric tuning provided by the choice of xanthene or dibenzofuran spacer or introduction of an aryl group trans to the spacer provides a homologous series of dicobalt(II) cofacial bisporphyrins spanning a wide range of vertical pocket sizes for further study.

Installation of a single rigid pillar into the cofacial bisporphyrin motif yields face-to-face systems where the motion of macrocyclic subunits with respect to each other is constrained to the vertical dimension (e.g., the Pacman effect); this vertical Pacman flexibility is critical for accommodating reaction intermediates during catalysis.[27,32,35−37] Comparative structural analysis of biszinc(II) and bisiron(III) μ-oxo complexes of DPD demonstrates that this platform can open and close its binding pocket by over 4 Å in metal−metal distances in the presence of suitable ligands.[34] An analogous intramolecular bisiron(III) μ-oxo complex is also obtained for the DPX template under similar conditions.[32]

To test whether the same type of Pacman effect would occur for cofacial platforms that contain an aryl group trans to the spacer, we prepared and crystallized the intramolecular bisiron(III) μ-oxo complex Fe_2O(DPXM) (**5**). Crystallographic data and selected geometrical measurements for the compound are provided in Tables 1 and 2, respectively. The structure of **5** is depicted in Figure 1. The clamping action of the porphyrin subunits in μ-oxo complex **5** is revealed by its reduced interplanar angle (IPA) of 25.4° and shortened metal−metal distance of 3.489 Å compared to the relaxed Zn_2(DPXM) compound (IPA = 32.9°, Zn−Zn = 5.913 Å).[33] The small torsional twist between porphyrin subunits in **5** (9.5°, defined as the torsion angle between the two meso-carbon−spacer bonds) confirms that the Pacman flexibility of the DPXM system is confined to the vertical direction. The compound exhibits a bent Fe−O−Fe angle of 155.2°. The five-coordinate iron atoms are raised 0.56 Å out of their respective 24-atom macrocyclic planes, though typical Fe−N (d_{avg} = 2.088 Å) and Fe−O (d_{avg} = 1.788 Å) distances are observed.

Table 2. Selected Bond Lengths (Å) and Angles (deg) for Fe_2O(DPXM) (**5**)

Bond Lengths (Å)			
Fe(1)−N(1)	2.081(5)	Fe(2)−N(5)	2.091(4)
Fe(1)−N(2)	2.084(4)	Fe(2)−N(6)	2.082(4)
Fe(1)−N(3)	2.085(5)	Fe(2)−N(7)	2.091(4)
Fe(1)−N(4)	2.099(4)	Fe(2)−N(8)	2.085(4)
Fe(1)−O(1)	1.786(3)	Fe(2)−O(1)	1.791(3)
Bond Angles (deg)			
O(1)−Fe(1)−N(3)	104.77(17)	O(1)−Fe(2)−N(5)	103.88(16)
O(1)−Fe(1)−N(4)	107.40(17)	O(1)−Fe(2)−N(7)	108.29(17)
N(3)−Fe(1)−N(4)	83.92(19)	N(5)−Fe(2)−N(7)	147.80(17)
O(1)−Fe(1)−N(2)	105.79(16)	O(1)−Fe(2)−N(6)	106.56(17)
N(3)−Fe(1)−N(2)	87.52(17)	N(5)−Fe(2)−N(6)	84.51(17)
N(4)−Fe(1)−N(2)	146.82(17)	N(7)−Fe(2)−N(6)	87.67(17)
O(1)−Fe(1)−N(1)	105.12(17)	O(1)−Fe(2)−N(8)	103.86(16)
N(3)−Fe(1)−N(1)	150.11(17)	N(5)−Fe(2)−N(8)	87.57(17)
N(4)−Fe(1)−N(1)	87.21(19)	N(7)−Fe(2)−N(8)	83.54(17)
N(2)−Fe(1)−N(1)	84.46(17)	N(6)−Fe(2)−N(8)	149.56(17)

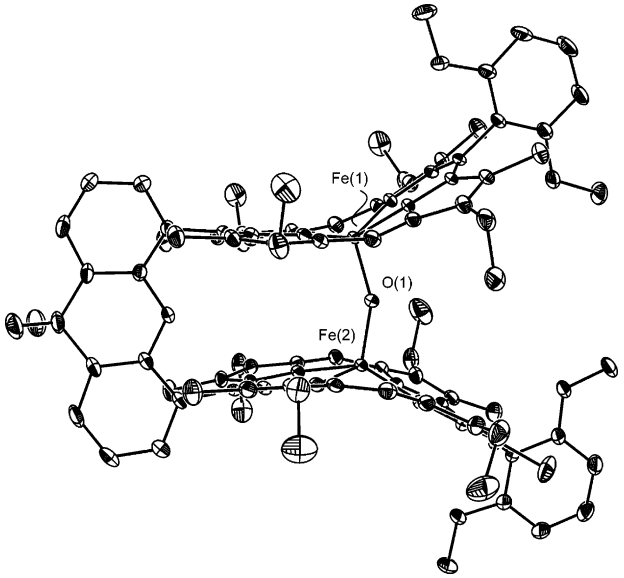

Figure 1. Crystal structure of **5**. Thermal ellipsoids are drawn at the 25% probability level. Hydrogen atoms have been omitted for clarity.

Compound **5** completes the structurally homologous series of open and closed forms of Pacman porphyrins shown in Figure 2. The structural comparison establishes that the introduction of an aryl group trans to the spacer does not greatly hinder the vertical Pacman flexibility of the cofacial platforms relative to their unsubstituted counterparts. More generally, the results of Figure 2 illustrate the ability of the cofacial porphyrins to clamp their "jaws" down on exogenous substrates for DPX or DPD bridges with or without trans-aryl substitution.

Electrochemistry. Electrochemical measurements of **1**−**4** verify that the redox properties of the parent DPX and DPD systems are not appreciably perturbed by introduction of an aryl group trans to the spacer. Table 3 lists the oxidative redox potentials of the dicobalt(II) bisporphyrin systems. Cyclic voltammograms of Co_2(DPXM) (**3**) exhibit two reversible one-

(35) Pistorio, B. J.; Chang, C. J.; Nocera, D. G. *J. Am. Chem. Soc.* **2002**, *124*, 7884−7885.
(36) Chang, C. J.; Loh, Z.-H.; Deng, Y.; Nocera, D. G. *Inorg. Chem.* **2003**, *42*, 8262−8269.
(37) Hodgkiss, J. M.; Chang, C. J.; Pistorio, B. J.; Nocera, D. G. *Inorg. Chem.* **2003**, *42*, 8270−8277.

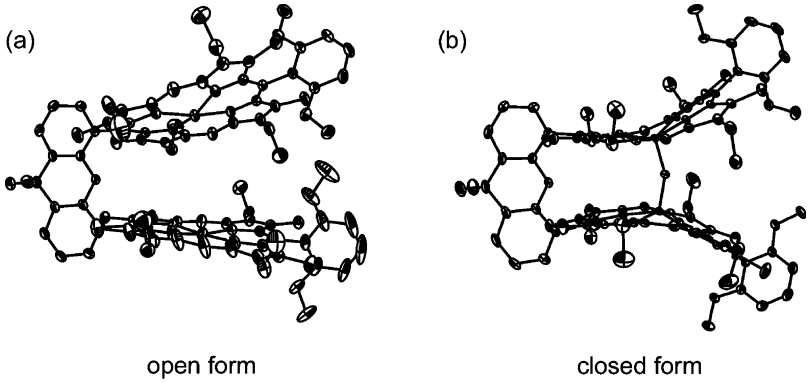

Figure 2. Comparative views of the open and closed forms of the Pacman DPXM platform, (a) Zn_2(DPXM) and (b) **5**, respectively. Hydrogen atoms have been omitted for clarity.

Table 3. Electrochemical and Electrocatalytic Data for Cofacial Bisporphyrins **1**−**4**

		electrocatalytic O_2 reduction	
	E_{ox}/V vs Ag/AgCl	E_{disk} vs Ag/AgCl	% H_2O product
1	+0.28, +0.17	+0.38	72
2	+0.33	+0.37	80
3	+0.31, +0.14	+0.24	52
4	+0.33	+0.25	46

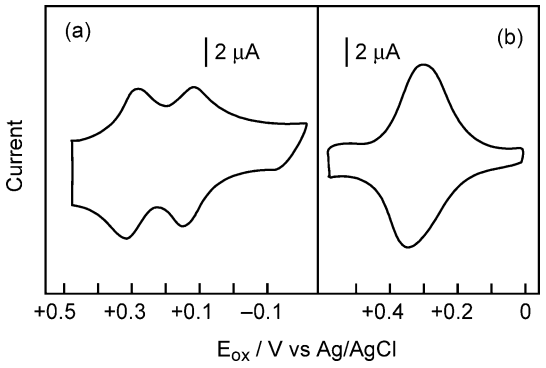

Figure 3. Thin-layer cyclic voltammograms for (a) **3** in tolunitrile and (b) **4** in nitrobenzene, using 0.1 M *n*-tetrabutylammonium perchlorate (TBAP) as a supporting electrolyte. Scan rate = 10 mV/s, potentials reported vs Ag/AgCl.

electron oxidation waves at +0.31 and +0.14 V vs Ag/AgCl (Figure 3a). The splitting of the oxidation processes arises from strong interactions between two proximate porphyrin π systems.[27,38−41] The mixed-valence behavior displayed by **3** is similar to what is observed for the parent complex, Co_2(DPX) (**1**), at comparable potentials (E° = +0.28 and +0.17 V).[27] Conversely, cyclic voltammograms of Co_2(DPDM) (**4**) give a single, reversible two-electron oxidative wave at a potential identical to that of Co_2(DPD) (**2**) (E° = +0.33 V, Figure 3b),[27] establishing that the porphyrinic subunits in the dibenzofuran-bridged platforms are too far apart to perturb each other electronically. These electrochemical data show that the redox behaviors of the DPXM and DPDM platforms mirror their corresponding DPX and DPD counterparts.

(38) Collman, J. P.; Hutchison, J. E.; Lopez, M. A.; Tabard, A.; Guilard, R.; Seok, W. K.; Ibers, J. A.; L'Her, M. *J. Am. Chem. Soc.* **1992**, *114*, 9869−9877.
(39) Guilard, R.; Lopez, M. A.; Tabard, A.; Richard, P.; Lecomte, C.; Brandès, S.; Hutchison, J. E.; Collman, J. P. *J. Am. Chem. Soc.* **1992**, *114*, 9877−9889.
(40) Le Mest, Y.; L'Her, M.; Saillard, J. Y. *Inorg. Chim. Acta* **1996**, *248*, 181−191.
(41) Le Mest, Y.; Inisan, C.; Laouenan, A.; L'Her, M.; Talarmain, J.; El Khalifa, M.; Saillard, J. Y. *J. Am. Chem. Soc.* **1997**, *119*, 6095−6106.

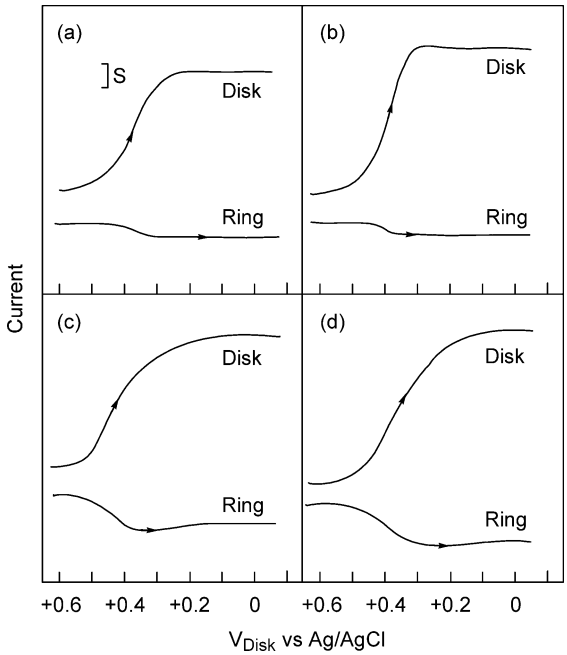

Figure 4. Rotating Pt ring−disk voltammograms for reduction of O_2 at pyrolytic graphite disks coated with (a) **1**, (b) **2**, (c) **3**, and (d) **4**. Rotation rate, 100 rpm; disk current, $S = 10\ \mu$A; ring current, $S = 5\ \mu$A; supporting electrolyte, 0.5 M $HClO_4$/1.5 M TFA saturated with air for **1** and **2**, 2 M $HClO_4$ saturated with air for **3** and **4**; ring held at +1.0 V vs Ag/AgCl.

Catalytic Reduction of O_2. We next sought to examine the effect of trans-aryl substitution on the selectivity for four-proton, four-electron versus two-proton, two-electron reduction of O_2 catalyzed by these Pacman motifs. To this end, complexes **1**−**4** were screened for their electrocatalytic activity for O_2 reduction in acidic media. Figure 4 displays current−potential responses for catalytic O_2 reduction at a rotating graphite disk/platinum ring electrode coated with **1**−**4**, and the results are collected in Table 3.

The parent DPX and DPD complexes are selective catalysts for the direct reduction of O_2 to H_2O over the more commonly observed pathway to produce H_2O_2. Co_2(DPX) (**1**) reduces O_2 at a potential of +0.38 V vs Ag/AgCl, with 72% selectivity for the four-proton, four-electron pathway to H_2O (Figure 4a), and Co_2(DPD) (**2**) catalyzes O_2 reduction at +0.37 V, with direct production of H_2O at 80% selectivity (Figure 4b).[27] In contrast, DPXM and DPDM complexes bearing a trans-aryl group display markedly lower H_2O/H_2O_2 product ratios than their parent DPX and DPD counterparts while exhibiting similar selectivities

compared to each other. Co_2(DPXM) (**3**) catalyzes O_2 reduction at +0.24 V, with 52% proceeding along the four-proton, four-electron pathway to produce H_2O (Figure 4c); Co_2(DPDM) (**4**) catalyzes O_2 reduction at +0.25 V, with 46% going directly to H_2O (Figure 4d). The catalytic studies clearly show that installation of a trans-aryl group into the Pacman motif results in decreased selectivity for the direct reduction of O_2 to H_2O, with a comparable effect for both xanthene- and dibenzofuran-bridged scaffolds. Because the structural flexibility and redox behavior of the cofacial bisporphyrin systems are largely unperturbed by trans-aryl substitution, more subtle electronic and proton-coupled effects are inferred for this change in catalytic selectivity.

Electronic Structure Calculations. Density functional theory (DFT) was applied to the parent (DPX) and trans-aryl-substituted (DPXM) derivatives of the $[Co_2(\text{bisporphyrin})(O_2)]^+$ in order to probe the origin of the diminished catalytic selectivity for O_2 to H_2O reduction by trans-aryl-substituted Pacman porphyrins. The object of these calculations was a Co(III)/Co(III) superoxo intermediate because experimental studies implicate this O_2-carrying species as the critical entry point into the catalytic O_2 reduction cycle.[38,41−43]

Geometry optimization of $[Co_2(DPX)(O_2)]^+$ with a doublet spin state affords a structure with the bridging O_2 adduct adopting an end-on geometry. To avoid complications arising from predisposed structural models,[41] no constraints were placed on O_2 binding in an end-on or side-on arrangement; in fact, the end-on structure is also obtained from an initial input geometry, using an idealized side-on $[Co_2O_2]$ core. The Co centers are displaced slightly out of the N_4 porphyrin mean plane (d_{avg} = 0.07 Å), giving a Co−Co distance of 4.35 Å, with Co−O bond lengths averaging 1.83 Å. The calculated O−O bond length of 1.35 Å is characteristic for a superoxo-bridged bimetallic unit (1.26−1.36 Å), resulting in a $[Co^{III}_2-(O_2^-)]$ configuration for the Pacman $[Co_2O_2]$ core. Mulliken population analysis reveals that the total spin density on the $[Co_2O_2]$ core is 1.068 e, suggesting that the majority of the unpaired spin density is localized on the $[Co_2O_2]$ unit. The results are in good agreement with the experimental observation of a 15-line EPR spectrum for $[Co_2(DPX)(O_2)(1,5\text{-dicyclohexylimidazole})_2]^+$ [27] and related μ-superoxodicobalt(III) complexes of cofacially strapped FTF4 and pillared DPB bisporphyrins.[38,41]

The optimized geometry of $[Co_2(DPXM)(O_2)]^+$ is similar to that of its DPX analogue. A doublet spin state produces a complex with an end-on O_2 adduct bridging the two Co centers. The Co−Co distance (4.50 Å) and average Co−O (1.88 Å) bond length for the DPXM monocation species compare favorably to values observed for the DPX analogue. The O−O bond length (1.32 Å) and unpaired spin density localized on the $[Co_2O_2]$ fragment (1.082 e total) for $[Co_2(DPXM)(O_2)]^+$ also support its assignment as a μ-superoxodicobalt(III) complex. In contrast to the DPX superoxo species, however, trans-aryl substitution results in significant nonplanar distortions of the porphyrin subunits within the DPXM superoxo cleft. For $[Co_2(DPXM)(O_2)]^+$, one porphyrin exhibits a ruffled-type conformation, whereas distortion of the other macrocycle is dominated by saddling. The average mean plane deviations for these macrocycles are 0.31 and 0.20 Å, respectively. The nonplanar distortions result in appreciably less effective charge transfer from the cobalt bisporphyrin fragment to the reduced O_2 substrate for $[Co_2(DPXM)(O_2)]^+$ (−0.237 e) compared to the parent DPX counterpart (−0.284 e) and also lead to stronger O−O bonding in the former. The Mulliken overlap populations for the O−O units in $[Co_2(DPXM)(O_2)]^+$ and $[Co_2(DPX)(O_2)]^+$ are +0.175 and +0.159 e, respectively.

The electronic and structural character of the highest occupied molecular orbital (HOMO), which is the site of proton transfer in acid−base reactions, is of greatest pertinence to O_2 reduction. Figure 5 illustrates significant differences between the HOMOs of the $[Co_2(DPX)(O_2)]^+$ and $[Co_2(DPXM)(O_2)]^+$ species. The singly occupied HOMO of the DPX superoxo species consists of localized molecular orbitals with significant π^*(Co−O) and π^*(O−O) character on the $[Co_2O_2]$ core, as well as a π-delocalized system of a_{1u} symmetry on one of the porphyrin macrocycles. The pronounced electron density on the superoxo indicates it to be basic and to be the target of proton transfer. Conversely, the singly occupied HOMO of $[Co_2(DPXM)(O_2)]^+$ consists solely of a porphyrin π system of a_{1u} symmetry, with no electron density observed on the superoxo. This electronic structure disfavors the targeted delivery of proton equivalents to the $[Co_2O_2]$ core.

Discussion

The selective conversion of O_2 to H_2O by heme/copper terminal oxidases is made possible by their ability to effectively balance proton and electron inventories. In particular, the bimetallic heme/Cu_B active site of COX mediates these PCET events through heme−oxygen intermediates that are analogous to those observed in monometallic heme proteins.[44] Viewed within a PCET framework,[45] the complete reduction of O_2 to H_2O requires four protons and four electrons for the cleavage of two formal O−O bonds, whereas the partial reduction of O_2 to H_2O_2 requires two protons and two electrons for the cleavage of a single formal O−O bond. Specific activation of the second O−O bond, which is the key determinant in producing H_2O instead of H_2O_2, is thus predicated on the proper delivery of additional proton equivalents to substrate bound within the reducing active site. In COX, spectroscopic and kinetics studies of partially and fully reduced enzymes establish that the O−O bond is broken upon the addition of three electrons and one proton.[46−49] We propose that this crucial proton and electron stoichiometry for O−O bond cleavage is preserved in the O_2 reduction reactivity displayed by cofacial bisporphyrins.

Scheme 1 presents a mechanistic model for the PCET activation of the O−O bond by Pacman porphyrins. Previous experimental studies have shown that the one- and two-electron oxidized cofacial platforms are capable of binding O_2, whereas the fully reduced $[Co_2(\text{bisporphyrin})]$ complex is unreactive to the O_2 substrate.[38,41,42] For the Pacman porphyrins reported here,

(42) Chang, C. K. *J. Chem. Soc., Chem. Commun.* **1977**, 800−801.
(43) Proniewicz, L. M.; Odo, J.; Goral, J.; Chang, C. K.; Nakamoto, K. *J. Am. Chem. Soc.* **1989**, *111*, 2105−2110.
(44) Babcock, G. T. *Proc. Natl. Acad. Sci. U.S.A.* **1999**, *96*, 12971−12973.
(45) Chang, C. J.; Chang, M. C. Y.; Damrauer, N. H.; Nocera, D. G. *Biochim. Biophys. Acta* **2004**, *1665*, 13−28.
(46) Hansson, Ö.; Karlsson, B.; Aasa, R.; Vänngård, T.; Malmström, B. G. *EMBO J.* **1982**, *1*, 1295−1297.
(47) Blair, D. F.; Witt, S. N.; Chan, S. I. *J. Am. Chem. Soc.* **1985**, *107*, 7389−7399.
(48) Morgan, J. E.; Verkhovsky, M. I.; Palmer, G.; Wikström, M. *Biochemistry* **2001**, *40*, 6882−6892.
(49) Blomberg, M. R. A.; Siegbahn, P. E. M.; Babcock, G. T.; Wikström, M. *J. Am. Chem. Soc.* **2000**, *122*, 12848−12858.

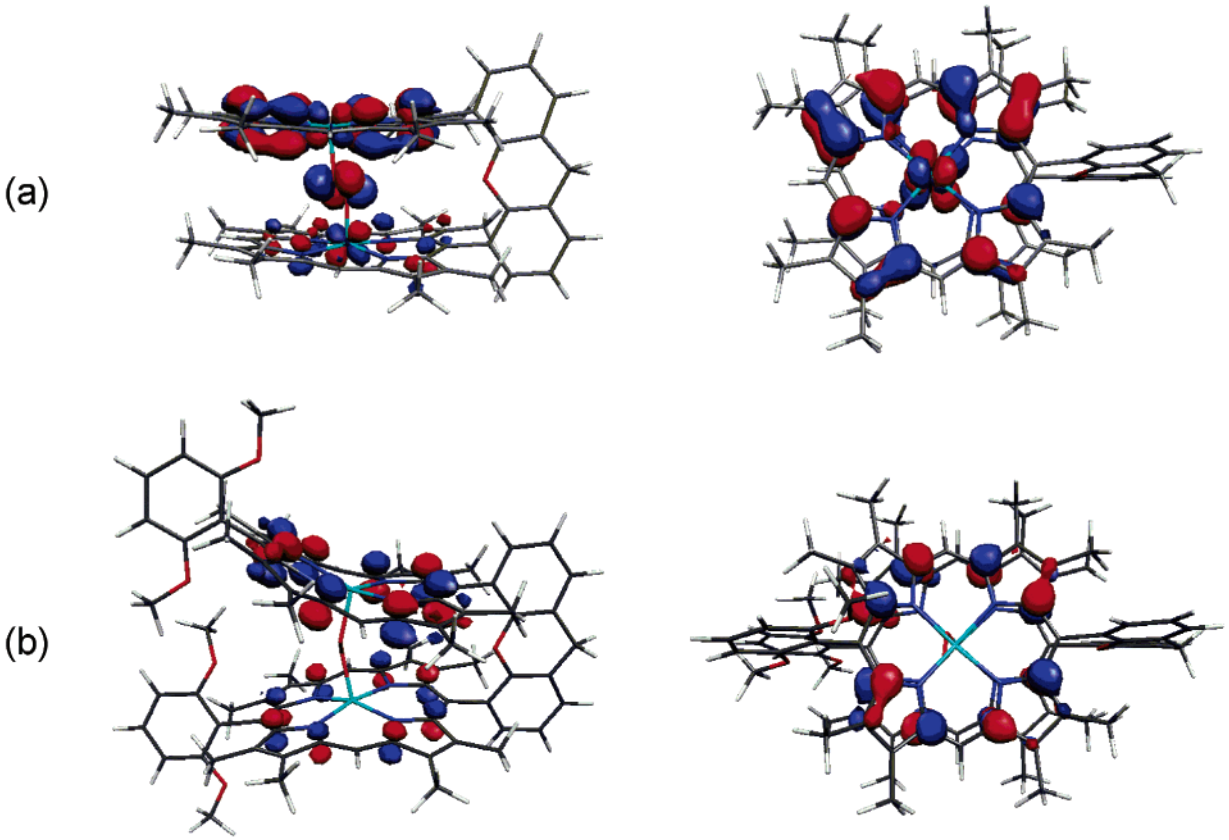

Figure 5. Singly occupied HOMOs of (a) $[Co_2(DPX)(O_2)]^+$ and (b) $[Co_2(DPXM)(O_2)]^+$. The structures on the left depict a side view, perpendicular to the bridge plane, whereas the structures on the right display a top view, perpendicular to the porphyrin planes.

EPR studies establish that the one-electron oxidized $Co^{II,III}_2$ cofacial porphyrin provides entry into the catalytic cycle. The $[Co_2(bisporphyrin)(O_2)]^+$ adduct formed from $Co^{II,III}_2$ and O_2 is stable to superoxide release and is poised for further reaction. Our results show that it is the basicity of the superoxo complex that is the key determinant of the selectivity for O_2 reduction. We propose that targeted proton transfer to the $[Co_2O_2]$ core of $[Co_2(bisporphyrin)(O_2)]^+$ triggers a multielectron transport process, bypassing one-electron processes to formal $[Co_2(bisporphyrin)(O_2)]$ peroxo-type intermediates that would favor H_2O_2 production. Protonation followed by a two-electron transfer provides the necessary equivalents to result in O−O bond cleavage. In this case, an oxo-hydroxy species, similar to the O−O bond cleavage product of COX,[9,46−48] would result; subsequent reduction by an additional electron produces the fully reduced product. We note however that a Co^{IV} oxo species may not be stable, and the system may drive through to the fully reduced product. If the superoxo is not sufficiently basic, inefficient proton transfer to $[Co_2(bisporphyrin)(O_2)]^+$ would result in either reversible loss of O_2 substrate or one-electron reduction to the peroxide level, with subsequent generation of H_2O_2. Thus, the key to the selective reduction of oxygen to water is the protonation state of the $[Co_2(bisporphyrin)(O_2)]^+$ monocation species; targeted proton delivery to the superoxo is essential for favoring multielectron over single-electron chemistry for specific O−O activation and cleavage.

The proposed scheme displayed in Figure 1 is appealing from several perspectives. As mentioned above, the proper stoichiometry of one proton and three electrons needed for O−O bond cleavage is satisfied. The superoxo provides an important regulatory function for oxygen activation by using a proton to mediate the transfer of the additional two electrons needed for O−O bond cleavage. In the absence of a proton, a single electron transfer yields the peroxide (a net two-electron transfer). In addition, the proton has the dual function of weakening the O−O bond upon protonation. The general model proposed in Scheme 1 also clarifies the perplexing observations of synthetic constructs that show similar or enhanced reactivity when the second coordination site is empty[29,30] or replaced by an appropriate Lewis acidic metal ion.[28] The role of the second functional site, whether that be another porphyrin, metal complex, or metal-free coordination sphere, is to adjust the pK_a of the oxygen adduct. Because a cooperative redox activity is not required, the site may be redox inactive or completely absent.

Concluding Remarks

We have investigated the effect of proton delivery on the catalytic selectivity of a homologous set of cofacial Pacman porphyrins. Our findings indicate that targeted proton transfer is critical for selecting the four-proton, four-electron pathway to H_2O over the more common two-proton, two-electron pathway to H_2O_2. The O_2-carrying $[Co_2(bisporphyrin)(O_2)]^+$ species of Pacman systems DPX and DPD targets proton transfer to the reducing $[Co_2O_2]$ core, favoring complete O−O cleavage to produce two H_2O molecules. In contrast, the superoxo adduct of trans-aryl DPXM and DPDM analogues disfavors protonation of the $[Co_2O_2]$ unit, resulting in a stronger O−O bond and increased production of H_2O_2.

The combined experimental and theoretical findings have important implications for the design of catalysts for specific

Scheme 1

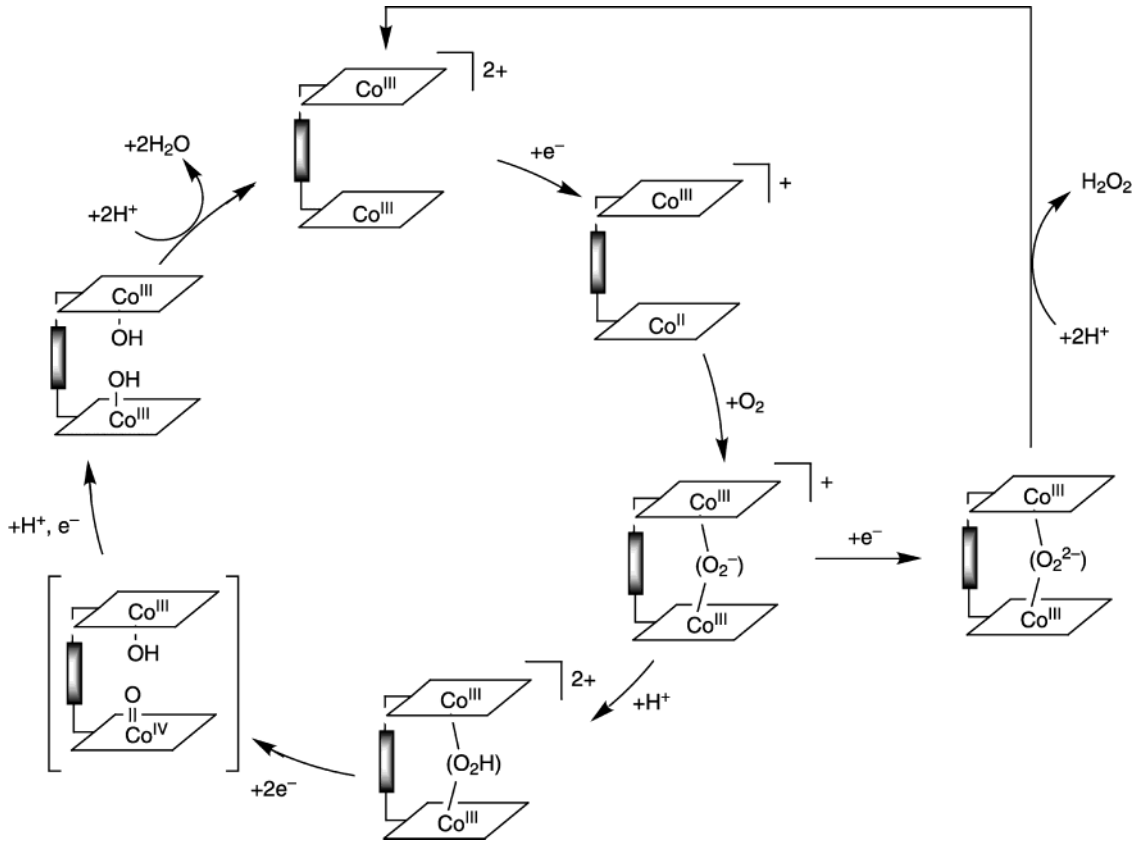

cleavage of O−O bonds. As discussed by Taube,[50] cofacial bisporphyrins fulfill the two general requirements for an effective four-electron, four-proton O_2 reduction catalyst: (i) the bypass of kinetically available one-electron routes through cooperative reactivity and (ii) the protection of peroxo-type intermediates against protonation and release. The substantial body of work on cofacial bisporphyrins as O_2 reduction catalysts has clarified the *structural* attributes of an effective architecture, including the restriction of macrocyclic subunits to a face-to-face arrangement with minimal lateral displacements, while allowing sufficient vertical flexibility to bind and activate the O_2 substrate.[26,27,51] Against this backdrop of expertise, we have now established the importance of a proper *electronic* environment for the bound O_2 substrate by directing proton transport. In particular, we find that targeted proton transfer is required for selective O−O reactivity and suggest that specific protonation of the O_2-carrying superoxo adduct bypasses the formation of peroxo-type adducts by facilitating multielectron processes. In closing, our results highlight the importance of proton transport and electronic structure in guiding catalytic O_2 reduction pathways. Along these lines, we are now testing the ability of monometallic Hangman constructs that control both proton and electron inventories[45,52−55] to catalyze selective O_2 activation chemistry.

Experimental Section

Materials. Aluminum oxide 60 (EM Science) was used for column chromatography. Analytical thin-layer chromatography was performed using JT Baker IB-F aluminum oxide (precoated sheets, 0.2 mm thick). Solvents for synthesis were of reagent grade or better and were dried according to standard methods. The Pacman porphyrins H_4(DPX),[31] H_4(DPD),[34] H_4(DPXM),[33] and H_4(DPDM)[33] were synthesized as described previously. All other reagents were used as received.

Co_2(DPX) (1). In a drybox, H_4(DPX) (120 mg, 0.10 mmol), anhydrous cobalt(II) chloride (200 mg), 2,6-lutidine (0.2 mL), and THF (120 mL) were loaded in a 250-mL round-bottom flask. The mixture was refluxed under nitrogen for 12 h. The solvent was removed in vacuo, and the residue was purified by flash column chromatography under an inert atmosphere (alumina, THF). Recrystallation from dichloromethane/methanol gave **1** as an analytically pure purple crystalline powder (121 mg, 95% yield). Anal. Calcd for $C_{79}H_{82}Co_2N_8O$: C, 74.24; H, 6.47; N, 8.77. Found: C, 73.86; H, 6.42; N, 8.71. HRFABMS (M^+) calcd for $C_{79}H_{82}Co_2N_8O$ *m*/*z*, 1276.528; found, 1276.526.

Co_2(DPD) (2). In a drybox, a 100-mL flask equipped with a condenser was charged with H_4(DPD) (50 mg, 0.045 mmol), 2,6-lutidine (0.1 mL), $CoCl_2$ (100 mg), THF (12 mL), and benzene (12 mL). The mixture was refluxed under nitrogen for 12 h. The solvent was removed in vacuo, and the residue was purified by flash column chromatography under an inert atmosphere (alumina, THF). Recrystallation from dichloromethane/methanol gave **2** as an analytically pure maroon crystalline powder (50 mg, 91% yield). Anal. Calcd for $C_{76}H_{76}Co_2N_8O$: C, 73.89; H, 6.20; N, 9.54. Found: C, 73.82; H, 6.26; N, 8.94. HRFABMS (M^+) calcd for $C_{76}H_{76}Co_2N_8O$ *m*/*z*, 1234.481; found, 1234.480.

Co_2(DPXM) (3). To a solution of H_4(DPXM) (105 mg, 0.073 mmol) in THF (15 mL) and benzene (10 mL) containing 2,6-lutidine (0.2 mL) was added $CoCl_2$ (200 mg). The resulting mixture was refluxed for 10 h under nitrogen and taken to dryness. The solvent was removed in vacuo, and the residue was purified by flash column chromatography under an inert atmosphere (neutral alumina, THF). Recrystallation from dichloromethane/methanol gave **3** as an analytically pure brick-red powder (110 mg, 97% yield). Anal. Calcd for $C_{95}H_{102}N_8O_5Co_2$: C,

(50) Taube, H. *Prog. Inorg. Chem.* **1986**, *34*, 607−625.
(51) Collman, J. P.; Wagenknecht, P. S.; Hutchison, J. E. *Angew. Chem., Int. Ed. Engl.* **1994**, *33*, 1537−1554.

73.63; H, 6.37; N, 7.23. Found: C, 73.77; H, 6.53; N, 6.84. HRFABMS (M^+) calcd for $C_{95}H_{102}N_8O_5Co_2$ *m*/*z*, 1548.632; found, 1548.633.

Co_2(DPDM) (4). To a solution of H_4(DPDM) (52 mg, 0.037 mmol) in THF (8 mL) and benzene (8 mL) containing 2,6-lutidine (0.1 mL) was added $CoCl_2$ (120 mg). The resulting mixture was refluxed for 15 h under nitrogen and taken to dryness. The solvent was removed in vacuo, and the residue was purified by flash column chromatography under an inert atmosphere (neutral alumina, THF). Recrystallation from dichloromethane/methanol gave **4** as an analytically pure blood-red powder (51 mg, 91% yield). Anal. Calcd for $C_{92}H_{92}N_8O_5Co_2$: C, 73.29; H, 6.15; N, 7.43. Found: C, 73.60; H, 6.49; N, 6.90. HRFABMS (M^+) calcd for $C_{92}H_{92}N_8O_5Co_2$ *m*/*z*, 1506.586; found, 1506.590.

Fe_2O(DPXM) (5). A mixture of H_4(DPXM) (45 mg, 0.031 mmol) and $FeBr_2$ (100 mg) in THF (7 mL) and benzene (5 mL) containing 2,6-lutidine (0.1 mL) was refluxed under nitrogen for 5 h. The reaction was opened to air, and the solvent was removed by rotary evaporation. The remaining residue was taken up in dichloromethane and vigorously stirred with a 0.5 N NaOH solution (20 mL) for 30 min. The organic phase was separated, washed with water (3 × 25 mL), dried over Na_2SO_4, and taken to dryness. Purification by column chromatography (basic alumina, 85:15 chloroform/ethyl acetate) followed by recrystallization from dichloromethane/hexanes afforded analytically pure **5** (45 mg, 92% yield) as a brown crystalline solid. Anal. Calcd for $C_{95}H_{102}N_8O_6Fe_2$: C, 73.16; H, 6.33; N, 7.19. Found: C, 73.01; H, 6.20; N, 7.06. HRFABMS ($[M - O]^+$) calcd for $C_{95}H_{102}N_8O_5Fe_2$ *m*/*z*, 1542.636; found, 1542.633.

General Details of X-ray Data Collection and Reduction. X-ray diffraction data were collected using a Siemens 3 circle diffractometer equipped with a CCD detector. Measurements were carried out at −90 °C using Mo Kα (λ = 0.71073 Å) radiation, which was wavelength selected with a single-crystal graphite monochromator. Four sets of data were collected, using ω scans and a −0.3° scan width. All calculations were performed using a PC workstation. The data frames were integrated to *hkl*/intensity, and final unit cells were calculated by using the SAINT v.4.050 program from Siemens. The structures were solved and refined with the SHELXTL v.5.03 suite of programs developed by G. M. Sheldrick and Siemens Industrial Automation, Inc., 1995.

X-ray Structure of Fe_2O(DPXM)·$4CH_2Cl_2$·C_6H_{14} (5). A 0.36 mm × 0.11 mm × 0.10 mm chocolate-colored crystal of plate morphology was obtained from slow diffusion of hexane into a dichloromethane solution of the compound. The crystal was coated in STP oil treatment and mounted onto a glass fiber. A total of 23 352 reflections were collected in the θ range 2.37−25.00°, of which 17 671 were unique (R_{int} = 0.0387). The Patterson method was used to locate the iron atoms; all remaining atoms were placed using the difference Fourier map. Hydrogen atoms were placed in calculated positions using a standard riding model and were refined isotropically. The largest peak and hole in the difference map were 1.554 and −0.787 e Å^{-3}, respectively. The least-squares refinement converged normally, giving residuals of $R1$ = 0.0858 and w$R2$ = 0.2103, with GOF = 1.051.

Physical Measurements. Staff at the University of Illinois Mass Spectrometry Laboratory carried out mass spectral analyses. Elemental analyses were performed at Michigan State University. Absorption spectra were obtained using a Cary-17 spectrophotometer, modified by On-Line Instrument Systems (OLIS) to include computer control, or a Spectral Instruments 440 Model spectrophotometer.

Electrochemical Apparatus and Procedures. Cylindrical pyrolytic graphite rods with the edges of the graphitic planes explosed (Union Carbide) were mounted to stainless steel shafts with heat-shrinkable polyolefin tubing (Alpha Wire). The exposed graphite disk had an area of 0.32 cm^2. Electrode pretreatment and catalyst loading were carried out using standard procedures.[56] Briefly, the pyrolytic graphite rods were polished with 600 grit SiC paper (3M), sonicated in purified water (MilliQ Plus), washed with acetone, and dried. Porphyrins were adsorbed on the electrode surface by means of a dip-coating procedure: the freshly polished electrode was dipped for 1 min in a 0.1 mM solution of the porphyrin in chloroform, removed, washed immediately with pure chloroform, and dried in air. The dry, coated electrodes were transferred to the aqueous supporting electrolytes and utilized immediately.

The commercial rotating graphite disk−platinum ring electrode (Pine Instruments) was polished with 0.3 μm alumina on microcloth. The collection efficiency of the rotating ring−disk electrode (RRDE) employed was 0.39, as established by measurements with the $Fe(CN)_6^{3-/4-}$ couple. The percentage of oxygen reduction proceeding along the four-electron pathway to produce water was calculated using the formula $f_{water} = [N - (i_R/i_D)]/[N + (i_R/i_D)]$ where f_{water} is the fraction of oxygen reduced to water, N is the collection efficiency of the RRDE, and i_R and i_D are the ring and disk currents, respectively.

Computational Methods. Density functional theory (DFT) calculations were carried out at the local density approximation (LDA) level of theory using the Amsterdam Density Functional program.[57−60] Part of the calculations were performed on a home-built Linux cluster consisting of 12 processors running in parallel. Gradient corrections were introduced by using the Becke exchange functional (B)[61] and the Perdew−Wang (PW91) correlation functional.[62] C and H were described by a Slater-type orbital double-ξ basis set augmented by one set of polarization functions. Co, N, and O atoms were described by a Slater-type orbital triple-ξ basis set augmented by one set of polarization functions. Non-hydrogen atoms were assigned a frozen core potential, treating as core the shells up to and including 2p for Co and 1s for C, N, and O. Calculations on the doublet spin state were performed within the unrestricted formalism. Population analyses were carried out using the Mulliken method. Two minor structural simplifications were made to the cobalt bisporphyrin models employed in the calculations: (i) ethyl groups on the porphyrin macrocycles were replaced with methyl groups and (ii) methyl groups on the xanthene pillar were replaced with hydrogens.

Acknowledgment. C.J.C. thanks the National Science Foundation and the MIT/Merck Foundation for predoctoral fellowships. Z.-H.L. gratefully acknowledges the benefits of the M.I.T. Undergraduate Research Opportunities Program (UROP) and the National Science and Technology Board (Singapore) for an undergraduate scholarship. The National Institutes of Health (GM 47274) and the National Computational Science Alliance (CHE020041N) provided funding for this work.

Supporting Information Available: X-ray crystallographic file (CIF format) for **5**. This material is available free of charge via the Internet at http://pubs.acs.org.

JA049115J

(52) Yeh, C.-Y.; Chang, C. J.; Nocera, D. G. *J. Am. Chem. Soc.* **2001**, *123*, 1513−1514.
(53) Chang, C. J.; Yeh, C.-Y.; Nocera, D. G. *J. Org. Chem.* **2002**, *67*, 1403−1406.
(54) Chang, C. J.; Chng, L. L.; Nocera, D. G. *J. Am. Chem. Soc.* **2003**, *125*, 1866−1876.
(55) Chng, L. L.; Chang, C. J.; Nocera, D. G. *Org. Lett.* **2003**, *5*, 2421−2424.
(56) Yuasa, M.; Steiger, B.; Anson, F. C. *J. Porphyrins Phthalocyanines* **1997**, *1*, 181−187.
(57) ADF2000.02; Vrije Universiteit Amsterdam: Amsterdam, The Netherlands, 1999.
(58) Baerends, E. J.; Ellis, D. E.; Ros, P. *Chem. Phys.* **1973**, *2*, 41−51.
(59) Te Velde, G.; Bickelhaupt, F. M.; Baerends, E. J.; Fonseca Guerra, C.; Van Gisbergen, S. J. A.; Snijders, J. G.; Ziegler, T. *J. Comput. Chem.* **2001**, *22*, 931−967.
(60) van Gisbergen, S. J. A.; Snijders, J. G.; Baerends, E. J. *Comput. Phys. Commun.* **1999**, *118*, 119−138.
(61) Becke, A. D. *Phys. Rev. A: At., Mol., Opt. Phys.* **1988**, *38*, 3098−3100.
(62) Perdew, J. P.; Wang, Y. *Phys. Rev. B: Condens. Matter Mater. Phys.* **1992**, *46*, 12947−12954.